Dimensionless Two-Vector Model Predictive Current -Torque Control of Induction motor drives

Qazwan Abdullah
Faculty of Engineering Technology,Universiti Tun Hussein Onn Malaysia,Pagoh, Muar, Johor, Malaysia..
gazwan20062015@gmail.com

Nabil Farah
Faculty of Engineering and Information Technology, University of Technology Sydney, NSW, Australia.
Nabil.Farah@student.uts.edu.au

Mustafa Sami Ahmed
Department of Communication Engineering, University of Technology-Iraq
mustafa.sa.ahmed@uotechnology.edu.iq

Nor Shahida Mohd Shah
Faculty of Engineering Technology,Universiti Tun Hussein Onn Malaysia,Pagoh, Muar, Johor, Malaysia.
shahida@uthm.edu.my

Mohammed Hamood Othman Ahmed
China University of Petroleum (CUP).
mohammedhamood1992@gmail.com

Mogeeb A. A. Mosleh
Faculty of Engineering & information technology - Taiz university.
Mogeebmosleh@taiz.edu.ye

Md Hairul Nizam Talib
Faculty of Electrical Engineering, Universiti Teknikal Malaysia Melaka, Melaka, Malaysia
hairul nizam@uthm.edu.my

2024 IEEE 34th Australasian Universities Power Engineering Conference (AUPEC) | 979-8-3503-7794-1/24/$31.00 ©2024 IEEE | DOI: 10.1109/AUPEC62273.2024.10807592

***Abstract*—Model predictive controls (MPCs) have gained significant attention in induction motor drives due to their simplicity, non-linear control capabilities, and multi-objective control. However, conventional MPCs often face performance issues, such as high starting torque and torque ripples in model predictive current control (MPCC), and slow dynamic response and high current ripples in model predictive torque control (MPTC). This paper proposes a novel model predictive current torque control (MPCTC) for induction motor drives, combining the strengths of MPCC and MPTC by evaluating two separate cost functions for torque and current to generate an optimal switching vector. The fuzzy decision-making (FDM) principle is employed to evaluate these cost functions in a dimensionless manner, eliminating the need for weighting factors. Additionally, to enhance steady-state performance, an additional voltage vector is generated based on the current cost function and applied alongside the first vector generated using FDM, with appropriate duty cycle control. The effectiveness of the proposed MPCTC is validated through simulation and quantitative analysis, demonstrating superior performance in balancing dynamic and steady-state responses, as well as torque and current performance, compared to conventional MPCC and MPTC.**

Keywords— MPC, MPCC, MPTC, MPCTC, torque, current, fuzzy decision making, two vector.

I. INTRODUCTION

AC machines are being used in numerous industrial and domestic applications, which consequently takes a large portion of the global energy consumption [1, 2]. Induction Machines (IMs) are among the most popular AC machines with a wide range of applications, such as electric vehicle, oil and gas excavations, mills and conveyors [3-5]. Hence, improving the machines design and/or their control schemes can increase the efficiency and save energy.

The IMs control (IMs drives) have evolved over the years, starting with scalar V/F control techniques, where the supply magnitude and frequency are controlled to maintain a constant V/F ratio[6, 7]. Later on, to achieve high-performance machine drives, vector control strategies were introduced based on the principle of torque and flux decoupling incorporating separately excited DC machine control [8, 9]. For decades, vector control by its two types field oriented control (FOC) and direct torque control (DTC) have been the most popular AC machines drives [10-16]. Although, vector control techniques have shown great performances for AC machines drives, system complexity, high torque ripples and current harmonics are some of their drawbacks, thus advanced control methods are introduced to overcome these flaws[17, 18].

Recently, MPC has attracted a wide range of researchers and industries due to its simple concept, easy implementation, non-linearity control, constraints inclusion and multi-variable control [19-21]. Compared to FOC, MPC eliminates the current control block and reduce the drive complexity. Also, for DTC the voltage vector selected from MPC is much accurate and efficient than the one selected form pre-defined switching table of DTC [22].Different MPC techniques have been developed for electrical machine drives. The most common types are model predictive torque control (MPTC) and model predictive current control (MPCC) [23, 24]. MPTC utilizes torque and flux as control variables, while MPCC uses stator currents. Both techniques predict the future behaviors of these variables based on the machine model to select an optimal switching vector using a predefined cost function [25, 26].

Conventional MPTC/MPCC methods face some challenges including high computational burden, variable switching frequency, high torque and flux ripples at steady state response, high current harmonics, parameters sensitivity and weighting factors selection. Furthermore, MPTC often produces high current ripples and/or an unsatisfactory transient response, while MPCC may exhibit a good dynamic

979-8-3503-7794-1/24/$31.00 ©2024 IEEE

response. However, MPCC can result in high starting torque and significant torque ripples [27, 28]. Therefore, various improvements have been considered to tackle these issues including time-delay compensation [29]., using two-three voltage vector at one sampling with duty cycle control [30-35], switching frequency regulation[36-38], weighting factor tuning/ elimination and using additional control technique such as sensorless control. However, these enhanced MPC methods often increase overall system complexity and tend to focus on either improving torque or current performance. Consequently, they may still demand significant computational resources and can experience high torque or current ripples along with slow dynamic responses.

This research proposes a dimensionless two vector model predictive current torque control (MPCTC) for IM drives. The proposed MPCTC combines the features of MPCC and MPTC by evaluating two separate cost functions to generate an optimal switching vector that minimize toque and current ripples. To eliminate the need of weighting factor, fuzzy decision making (FDM) principle is used to evaluate the torque and current cost functions in a dimensionless manner. To further improve the steady-state performance, an additional voltage vector is generated based on current cost function and applied along with the first vector generated using FDM at each control cycle. The duty cycles of the first and additional voltage vector are determined based on the current and torque errors to ensure minimum torque and current ripples. The proposed MPCTC is validated through simulation and quantitative analysis and comparison with conventional MPCC and MPTC.

The remainder of the paper is organized as follows: Section II covers the modeling of conventional MPCs, Section III details the formulation of MPCTC, Section IV presents simulation results, quantitative analysis, and comparisons with conventional MPCs. Finally, Section V concludes by summarizing the findings and highlighting the contributions of this research.

II. Conventional MPCs

MPC can be categorized into two different types based on the controlled variables [35]. Model predictive current control (MPTC) is a type of MPC which controls and predicts the stator current. Another type is model predictive torque control (MPTC) which controls and predicts the torque and flux of the machine. In this section, the conventional MPCC and MPTC methods are discussed.

A. MPCC

MPCC is an effective MPC control method which utilizes stator currents as the controlled variables to control an electrical machine drive [37]. MPCC incorporates the principle of field-oriented control (FOC). The block diagram of MPCC for IM drives is shown in Fig. 1, which involves variables estimation, prediction, and cost function optimization. IM voltage and flux linkage equations are:

$$v_s = R_s i_s + \frac{d\varphi_s}{dt} \quad (1)$$

$$v_r = R_r i_r + \frac{d\varphi_r}{dt} \quad (2)$$

$$\varphi_s = L_s i_s + L_m i_r \quad (3)$$

$$\varphi_r = L_m i_s + L_r i_r \quad (4)$$

The state space equation of the motor current can be expressed as follows:

$$\frac{d}{dt}\begin{bmatrix} \mathrm{i_s} \\ \mathrm{i_r} \end{bmatrix} = \frac{1}{\sigma LsLr}\begin{bmatrix} -R_sL_r - j\omega_m L_m^2 & R_rL_m - j\omega_m L_m L_r \\ R_sL_m + j\omega_m L_m L_s & -R_rL_s + j\omega_m L_s L_r \end{bmatrix}\begin{bmatrix} \mathrm{i_s} \\ \mathrm{i_r} \end{bmatrix} + \frac{1}{\sigma LsLr}\begin{bmatrix} L_r & -L_m \\ -L_m & L_r \end{bmatrix}\begin{bmatrix} v_s \\ v_r \end{bmatrix} \quad (5)$$

Where v_s and v_s are the stator and rotor voltages, while the i_s and i_r are the stator and rotor currents. φ_s and φ_r are the stator and rotor flux component. R_s , R_r are the stator and rotor resistances. L_s and L_r denote stator and rotor inductance respectively, L_m is the mutual inductance, ω_r is the rotor speed.

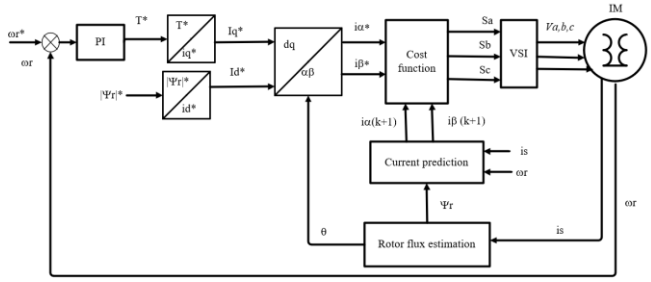

Fig.1. A diagram of MPCC for IM drives [47]

Based on the measured stator current, i_s, and rotor speed, ω_r, the stator flux (φ_s) can be estimated by rearranging (1) and applying forward Euler approximation which gives:

$$\varphi_s(k) = \varphi_s(k-1) + T_s\,[R_s i_s(k) - v_s(k)] \quad (6)$$

For the rotor flux (φ_r) it can be estimated by substituting the rotor current (i_r) in (4) into (3) and rearranging yields:

$$\varphi_r(k) = \varphi_s(k)\frac{\mathrm{L_r}}{\mathrm{L_m}} + \mathrm{i_s}(k)\left(\mathrm{L_m} - \frac{\mathrm{L_s L_r}}{\mathrm{L_m}}\right) \quad (7)$$

MPCC method predicts the stator current and evaluates it with reference current generated from the outer speed loop for all possible voltage vectors. From (5), the stator current is expressed as follows:

$$\frac{\mathrm{di_s}}{dt} = \frac{1}{\sigma LsLr}\left[-(R_sLr - \frac{R_rLm^2}{\mathrm{L_r}})\mathrm{i_s} - (j\omega_m Lm + \frac{R_rLm^2}{\mathrm{L_r}})\varphi_r + Lrv_s\right] \quad (8)$$

Using Euler forward method, the stator current at an instant (k+1) with sampling time Ts can be obtained as:

$$i_s(k+1) = i_s + \frac{T_s}{\sigma LsLr}\left[-(R_sL_r - \frac{R_rLm^2}{\mathrm{L_r}})\mathrm{i_s}(k) - (j\omega_m Lm + \frac{R_rLm^2}{\mathrm{L_r}})\varphi_r(k) + L_r\, v_s(k)\right] \quad (9)$$

MPCC works by measuring the actual values of stator currents (i_s) and rotor speed (ω_r), then use these values to estimates the values of rotor flux (φ_r) and predicts the future values of stator currents ($i_s(k+1)$) at the next sampling instant ($\mathrm{k}+1$). Using a cost function, the predicted values of stator currents ($i_s(k+1)$) are compared with a reference currents values (${i^*}_s$) generated from the outer speed control loop. The predication is achieved for all the feasible switching states of the inverter (i.e. 7 states for 2-level VSI), and the one that minimizes the cost function is selected as the optimum voltage vector. This voltage vector is directly applied as the switching signal to trigger the IGBT of the VSI so that the equivalent voltage is supplied to the motor. The general cost function used for MPCC can be expressed in the following equation:

$$g_j^{MPTC} = \sum_{h=1}^{N}\{|i_s^* - i_s(k+h)_j|\} \quad (10)$$

Where, g_j is the cost function for feasible switching states ($j = 7$ for 2L-VSI) and h is the prediction step number and N is the total prediction steps.

B. MPTC

MPTC/MPFC utilizes the flux and torque as the control variables [35]. The general block diagram of MPTC is shown in Fig. 2, which involves estimation of the variables that cannot be measured (flux) using the data of measured variables (current, speed), prediction of torque and flux for the next time interval (k+1), and cost function optimization. Similar to MPCC, the stator flux φ_s and rotor flux φ_r in MPTC can be estimated using the available data (measured variables) stator currents (i_s) and rotor speed (ω_r). The same equations (6) and (7) used in MPCC to estimates φ_s and φ_r can be used in MPTC.

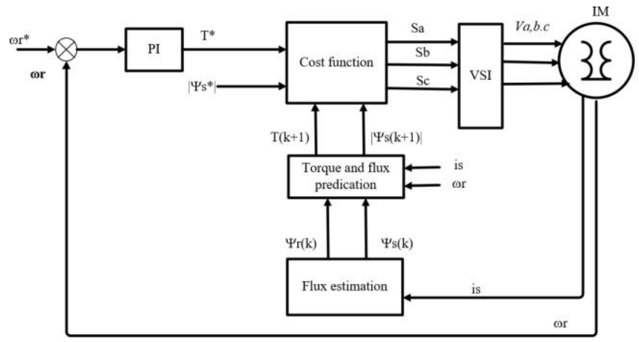

Fig.2. A diagram of MPTC for IM drives [49]

For torque prediction T at $(k+1)$, it depends on the stator flux and current predictions as:

$$\mathrm{T_e}(k+1) = \frac{3}{2}P\, Im\{\varphi_s(k+1)\, i_s(k+1)\} \quad (11)$$

The stator current can be predicted with the same equation used in MPCC (9).

Similar to MPCC, the stator currents and rotor speed are measured, then these measurements are used to estimate the stator and rotor flux. Then the future values of torque and flux at the next sampling instant (K+1) are predicted. With the help of a cost function, the predicted torque and flux values are compared with a reference torque and flux from the outer speed loop. An optimum voltage vector is selected based on the minimization of the cost function. The cost function of MPTC is expressed as:

$$g_j^{MPTC} = \sum_{h=1}^{N}\{|T_e^* - \mathrm{T_e}(k+h)_j| + \gamma|\varphi^* - \varphi(k+h)_j|\} \quad (12)$$

Since torque and flux are different in amplitude and unit, a proper weighting factor γ to be used. Most literature considers the weighting factor as the division of nominal torque over the nominal flux as $\gamma = \frac{T^*}{\varphi^*}$. [25].

III. PROPOSED DIMENSIONLESS TWO-VECTOR MPCTC

The performance of the conventional MPTC is limited by its slow dynamic response and high current ripples. On the other hand, conventional MPCC is constrained by high torque ripples and high starting torque. To address these issues, this paper proposes a Model Predictive Current and Torque Control (MPCTC) strategy that combines the features of both MPTC and MPCC. This approach evaluates both torque and current cost functions based on the predicted torque and currents with delay compensation. at $(k+2)$, as follows:

$$g_T = |T_e^* - T_e(k+2)| \quad (13)$$

$$g_C = |i_s^* - i_s(k+2)| \quad (14)$$

The cost functions in (13) and (14), incorporate two objective functions based on torque and current. These objective functions have varying degrees of importance and differ in magnitude and units. Hence, a weighting factor is necessary to balance the performance. However, selecting an appropriate weighting factor can be ambiguous and significantly impact performance if chosen incorrectly. To eliminate the need for a weighting factor, this paper employs fuzzy decision-making (FDM) to generate dimensionless decision functions for torque and currents.

FDM relies on the relative importance of each objective function and can be determined based on the decision maker's subjective and qualitative experience and judgment. FDM is particularly useful when there is insufficient or incomplete data for the solution[32]. While it differs slightly from traditional fuzzy approaches, FDM has been introduced for MPC in previous studies in power converters and induction motors. Furthermore, [31] utilized FDM to eliminate the weighting factors in conventional MPTC for PMSM drives. To apply FDM in MPC, it is necessary to specify membership and decision functions. The linear membership function is commonly used in MPC. When evaluating a cost function at different voltage vectors $g_i(V_s)$, $(V_s = 0-7)$, the linear membership function can be expressed as follows:

$$\mathrm{m_i}(V_s) = \left(\frac{g_i^{max} - g_i(V_s)}{g_i^{max} - g_i^{min}}\right)^{R_i} \quad (15)$$

where R_i is a priority weight factor that is determined based on the relative importance of each objective function. Typically, an intermediate (equal) value is assigned to both objective functions or a pairwise comparison matrix is constructed by comparing the objective functions against each other to derive the priority weight factor for each. Various relative importance cases are listed and assigned based on the priority of one objective function over another, as discussed in [29].The comparison matrix Γ between the two objective functions can be obtained as follows:

$$\Gamma = \begin{bmatrix} 1 & 3 \\ \frac{1}{3} & 1 \end{bmatrix} \quad (16)$$

By computing the eigenvector γ corresponding to the maximum value of the eigenvalues of Γ, the priority weight R_i can be expressed as:

$$R_i = [\,R_1 \;....\; R_i\,] = \frac{\gamma_{i\,max}}{\sum_{i=1}^{i}\gamma_{i\,max}} \quad (17)$$

For the proposed MPCTC, the current objective function is given moderate importance over the torque objective function to improve the current performance. Therefore, the priority weight $R_i = [R_T \;\; R_C]$, which has been obtained as $R_T = 0.4$ and $R_C = 0.6$. More discussion on how to construct the comparison matrix and compute the priority weight can be found in [27]. The membership function of the torque objective function $\mathrm{m_T}(V_s)$, and the current objective function $\mathrm{m_C}(V_s)$ can be represented as:

$$\mathrm{m_T}(V_s) = \left(\frac{g_T^{max} - g_T(V_s)}{g_T^{max} - g_T^{min}}\right)^{R_T} \quad (18)$$

$$\mathrm{m_C}(V_s) = \left(\frac{g_C^{max} - g_C(V_s)}{g_C^{max} - g_C^{min}}\right)^{R_C} \quad (19)$$

The cost functions of torque $g_T(V_s)$ and flux $g_C(V_s)$ are evaluated based on eight different voltage vectors($V_s = 0 - 7$) . Then, using the obtained values, their maximum (g_T^{max}, g_C^{max}), and minimum values (g_T^{min}, g_C^{min}) as in (18) and (19), the torque and current membership functions ($\mathrm{m_T}, \mathrm{m_C}$) in the range of [0 1] are obtained. Thus, an optimum voltage vector can be selected by minimizing and maximizing a decision function as:

$$\mathrm{m_D}(V_s) = \min\{m_T(V_s), m_C(V_s)\} \quad (20)$$

The optimum voltage vector (V_{opt}) is selected as:

$$V_{opt} = \max_{s=0-7}\left(\mathrm{m_D}(V_s)\right) \quad (21)$$

To improve the steady state response, the proposed MPCTC utilizes two switching vectors over one control cycle. The first vector, V_1, is obtained using FDM as in (21). while the second vector, V_2, is obtained by evaluating the current cost function in (14) based on eight voltage vectors ($V_0 - V_7$) of a 2-level three-phase inverter and minimizing it to obtain a second optimum voltage vector V_2 as follows:

$$V_2 = \min_{s=0-7}(\mathrm{g_C})$$

Thus, with two obtained voltage vectors $V_1$and V_2, the dq voltages components can be computed as follows:

$$u_{dq_1} = u_{dq}(V_1) \quad (22)$$

$$u_{dq_2} = u_{dq}(V_2) \quad (23)$$

The final reference voltage u_{dq}^{ref} is obtained as the combinations of the dq voltages components of two vectors with different duty cycles as:

$$u_{dq}^{ref} = \frac{t_1 \times u_{dq_1}}{T_s} + \frac{(T_s - t_1) \times u_{dq_2}}{T_s} \quad (24)$$

where T_s is the sampling time, and t_1 ($0 < t_1 < T_s$) is the time assigned for the first vector (V_1). The duty cycle d_1 of V_1 is determined based on the current error as:

$$d_1 = \left|\frac{i_s^* - i_s(k+2)}{C}\right| \quad (25)$$

where C is a positive constant value to be chosen to minimize the current ripple.

The proposed MPCTC eliminates the need for a weighting factor by transforming the torque and current objective functions into dimensionless quantities using FDM to obtain the first optimum voltage vector. To enhance steady-state performance and reduce current ripples, a second vector is applied alongside the optimum vector during each control cycle. This second vector, determined by evaluating the current cost function, is adjusted based on the current error. If the current ripple is high, the second vector (V_2) is applied for a longer duration to minimize the ripple.

To regulate the switching frequency and balance steady-state performance, a PWM modulator-based space vector is used. The reference u_{dq}^{ref} from (25) is fed to the SVM PWM modulator, generating the inverter's switching pulses with a regulated frequency. Figure 3 illustrates the block diagram of the proposed MPCTC.

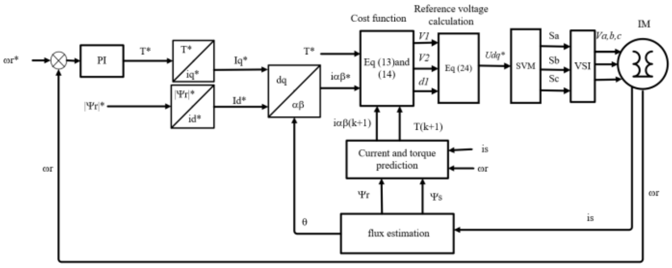

Fig.3. Proposed MPCTC for IM drives

IV. SIMULATION AND ANALYSIS

To validate the theoretical principles of the proposed MPCTC, a simulation analysis and performance comparison with conventional MPTC and MPCC were conducted based on an IM drive system. MATLAB/ Simulink software was used to develop the IM drive system incorporating MPCTC, MPTC, and MPCC with a 2.2 kW, 1400 rpm, 10 Nm IM, whose parameters are shown in Table I. The performance of MPCTC, MPCC, and MPTC was evaluated at the rated speed of 1400 rpm, both with and without load torque disturbances. Figure 4 illustrates the rotor speed, stator current, and electromagnetic torque performance of the three control schemes during no-load operations at rated speed. Additionally, Figure 5 demonstrates the performance of the control schemes at rated speed with a 10 Nm load disturbance applied at 2 seconds during forward operation and at 4 seconds during reverse operation.

The proposed MPCTC has demonstrated superior performance compared to conventional MPCC and MPTC in both transient and steady-state operations. MPCTC provides a better dynamic response and improved current performance compared to MPTC, along with lower starting torque and better torque response compared to MPCC. The proposed MPCTC balances torque and current performance, enhancing the IM drive's dynamic response while maintaining good steady-state performance.

TABLE I. PARAMETERS OF IM

Parameter	Value
Rated Voltage	537 Vdc
Poles	4
Frequency	50Hz
Rated Speed	1430 rpm
Stator Resistance	3.45 Ω
Rotor Resistance	3.6141 Ω
Stator Inductance	0.3246 H
Rotor Inductance	0.3252 H
Magnetizing Inductance	0.3117 H
Inertia	0.02 kgm^2
Viscous Friction	0.001 Nm/(rad/s)

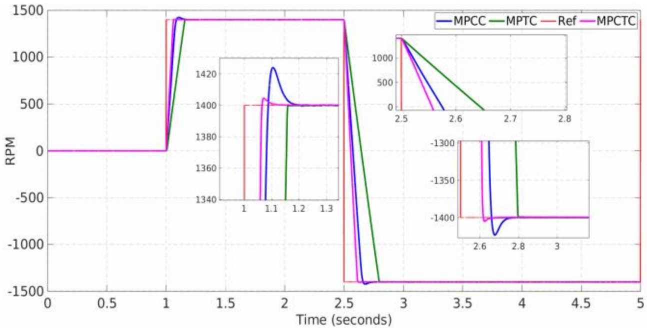

(a)

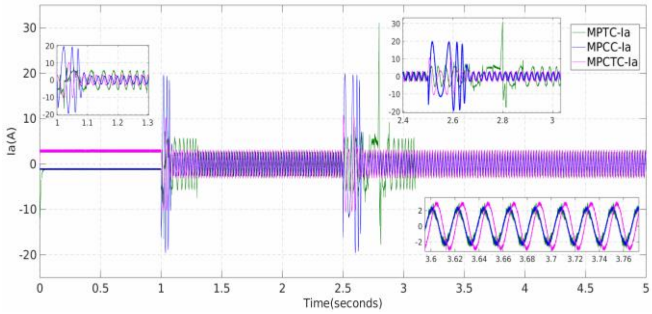

(b)

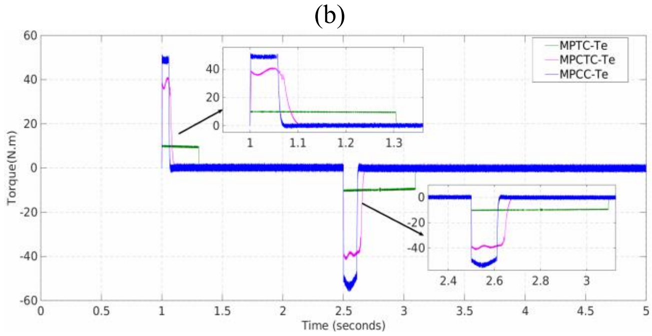

(c)

Fig.4. Performance comparison of proposed MPCTC and conventional MPTC and MPCC at rated speed (1400 rpm) and no-load,(a) speed response, (b) current response, and (c) torque response.

To gain better insight into the performance of MPCTC, a numerical quantitative comparison of transient and steady-state response characteristics was conducted. The properties of settling time (T_s), overshoot (OS), speed, current and torque steady-state ripples, and speed drop and recovery time due to load disturbance were computed for MPCTC, MPCC, and MPTC, as shown in Table II. At start-up, the speed increases from 0 to the rated speed of 1400 rpm, and Ts and OS are obtained. At 2 seconds of 1400 rpm steady-state speed, a 10 Nm load is applied, and the amount by which the speed drops below 1400 rpm is computed as the speed drop, and the time it takes to return to the steady-state speed of 1400 rpm is computed as the recovery time. The speed, current and torque steady-state ripples are computed for 0.5s (N=10000) of steady-state signals at 1400 rpm with 10 Nm. Generally, a steady-state ripple of a signal can be computed based on the following:

$$x_{ripple} = \sqrt{\frac{1}{N}\sum_{i=1}^{N}(x_i^* - x_i)^2} \tag{26}$$

where N is the number of samples, x_i^* and x_i are the reference and actual signals which can be the speed, current and torque signals.

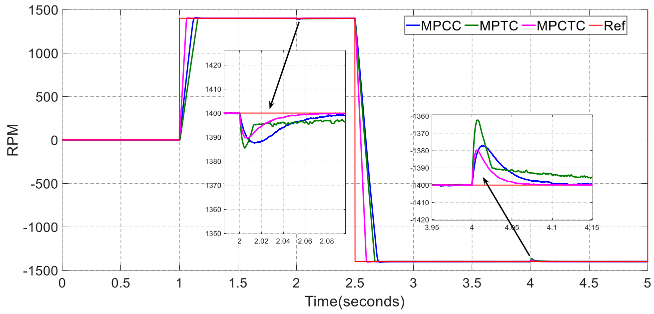

(a)

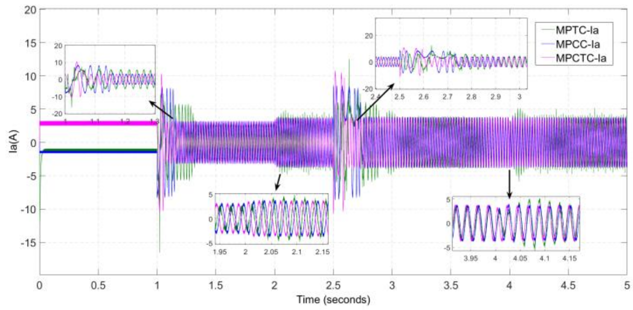

(b)

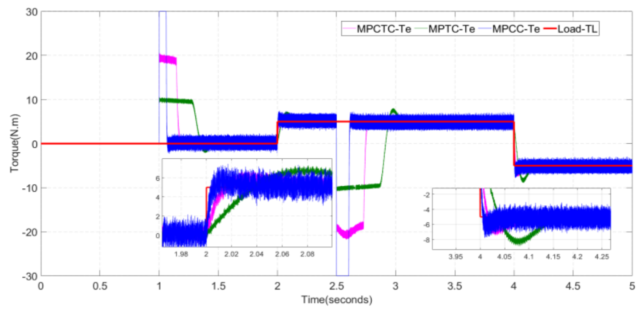

(c)

Fig.5. Performance comparison of proposed MPCTC and conventional MPTC and MPCC at rated speed (1400 rpm) with load disturbance,(a) speed response,(b) current response, and (c) torque response.

TABLE II. NUMERICAL COMPARISON OF MPCS AND FOC &DTC AT RATED SPEED 1400 RPM

Method Measure	MPCC	MPTC	MPCTC
Overshoot (%)	1.17	0.57	0.71
Rise Time (S)	0.098	0.133	0.062
Settling Time (S)	0.094	0.157	0.078
Speed ripple (rpm)	2.780	3.231	2.354
Torque ripple (Nm)	1.341	0.864	0.754
Current ripple (A)	0.963	1.532	0.931
Speed drop (rpm)	15	18	11
Recovery Time (S)	0.121	0.187	0.093

The numerical comparison of MPCTC, MPCC, and MPTC highlights MPCTC's superior performance across various metrics. MPCTC exhibits the fastest rise time (0.062 s) and shortest settling time (0.078 s), indicating a quick and stable dynamic response. It maintains the lowest speed ripple (2.354 rpm), torque ripple (0.754 Nm), and current ripple (0.931 A), ensuring smooth and efficient steady-state operation. Additionally, MPCTC shows the smallest speed drop (11 rpm) and the fastest recovery time (0.093 s) under load disturbances, outperforming both MPCC and MPTC. These results demonstrate that MPCTC provides a balanced and improved performance in both transient and steady-state conditions.

V. Conclusion

Conventional MPCC is constrained by unsatisfactory torque performance, while conventional MPTC is limited by slow dynamic response and high current ripples. To address these issues, this paper proposed a novel MPC control scheme (MPCTC) that combines the features of MPCC and MPTC. The proposed MPCTC evaluates both torque and current cost functions and utilizes fuzzy decision-making (FDM) to eliminate the need for a weighting factor. Furthermore, two switching vectors, along with space vector PWM, are employed to improve steady-state response and regulate switching frequency. The proposed MPCTC demonstrates superior performance compared to both MPCC and MPTC, achieving a balanced improvement in torque and current performance.

References

[1] R. Saidur, S. Mekhilef, M. B. Ali, A. Safari, and H. A. Mohammed, "Applications of variable speed drive (VSD) in electrical motors energy savings," *Renewable and Sustainable Energy Reviews,* vol. 16, no. 1, pp. 543-550, 2012/01/01/ 2012.

[2] V. Kazakbaev, V. Prakht, V. Dmitrievskii, S. Sarapulov, and D. Askerov, "Comparison of power consumption of synchronous reluctance and induction motor drives in a 0.75 kW pump unit," in 2017 International Siberian Conference on Control and Communications (SIBCON), 29-30 June 2017 2017, pp. 1-6.

[3] X. Liang and O. Ilochonwu, "Induction Motor Starting in Practical Industrial Applications," *IEEE Transactions on Industry Applications,* vol. 47, no. 1, pp. 271-280, 2011.

[4] C. B. Jacobina, M. B. d. R. Correa, E. R. C. d. Silva, and A. M. N. Lima, "Induction motor drive system for low-power applications," *IEEE Transactions on Industry Applications,* vol. 35, no. 1, pp. 52-61, 1999.

[5] H. H. Eldeeb, H. Zhao, and O. A. Mohammed, "Detection of TTF in Induction Motor Vector Drives for EV Applications via Ostu's-Based DDWE," *IEEE Transactions on Transportation Electrification,* pp. 1-1, 2020.

[6] A. Munoz-Garcia, T. A. Lipo, and D. W. Novotny, "A new induction motor V/f control method capable of high-performance regulation at low speeds," *IEEE Transactions on Industry Applications,* vol. 34, no. 4, pp. 813-821, 1998.

[7] K. Koga, R. Ueda, and T. Sonoda, "Constitution of V/f control for reducing the steady-state speed error to zero in induction motor drive system," *IEEE Transactions on Industry Applications,* vol. 28, no. 2, pp. 463-471, 1992.

[8] M. P. Kazmierkowski and A. B. Kasprowicz, "Improved direct torque and flux vector control of PWM inverter-fed induction motor drives," *IEEE Transactions on Industrial Electronics,* vol. 42, no. 4, pp. 344-350, 1995.

[9] D. W. Novotny and T. A. Lipo, *Vector control and dynamics of AC drives*. Oxford university press, 1996.

[10] K. Wang, Y. Li, Q. Ge, and L. Shi, "An Improved Indirect Field-Oriented Control Scheme for Linear Induction Motor Traction Drives," *IEEE Transactions on Industrial Electronics,* vol. 65, no. 12, pp. 9928-9937, 2018.

[11] M. Moallem, B. Mirzaeian, O. A. Mohammed, and C. Lucas, "Multi-objective genetic-fuzzy optimal design of PI controller in the indirect field oriented control of an induction motor," *IEEE Transactions on Magnetics,* vol. 37, no. 5, pp. 3608-3612, 2001.

[12] Z. Daboussi and N. Mohan, "Digital simulation of field-oriented control of induction motor drives using EMTP," *IEEE Transactions on Energy Conversion,* vol. 3, no. 3, pp. 667-673, 1988.

[13] N. Farah *et al.*, "A Novel Self-Tuning Fuzzy Logic Controller Based Induction Motor Drive System: An Experimental Approach," *IEEE Access,* vol. 7, pp. 68172-68184, 2019.

[14] Z. Zhang, R. Tang, B. Bai, and D. Xie, "Novel Direct Torque Control Based on Space Vector Modulation With Adaptive Stator Flux Observer for Induction Motors," *IEEE Transactions on Magnetics,* vol. 46, no. 8, pp. 3133-3136, 2010.

[15] Y. N. Tatte and M. V. Aware, "Torque Ripple and Harmonic Current Reduction in a Three-Level Inverter-Fed Direct-Torque-Controlled Five-Phase Induction Motor," *IEEE Transactions on Industrial Electronics,* vol. 64, no. 7, pp. 5265-5275, 2017.

[16] S. Kuo-Kai, S. Li-Jen, C. Hwang-Zhi, and J. Ko-Wen, "Flux compensated direct torque control of induction motor drives for low speed operation," *IEEE Transactions on Power Electronics,* vol. 19, no. 6, pp. 1608-1613, 2004.

[17] F. Wang, Z. Zhang, X. Mei, J. Rodríguez, and R. Kennel, "Advanced control strategies of induction machine: Field oriented control, direct torque control and model predictive control," *Energies,* vol. 11, no. 1, p. 120, 2018.

[18] N. Farah *et al.*, "Analysis and investigation of different advanced control strategies for high-performance induction motor drives."

[19] S. Mariethoz, A. Domahidi, and M. Morari, "High-Bandwidth Explicit Model Predictive Control of Electrical Drives," *IEEE Transactions on Industry Applications,* vol. 48, no. 6, pp. 1980-1992, 2012.

[20] S. Vazquez *et al.*, "Model predictive control: A review of its applications in power electronics," *IEEE industrial electronics magazine,* vol. 8, no. 1, pp. 16-31, 2014.

[21] J. Rodriguez *et al.*, "State of the art of finite control set model predictive control in power electronics," *IEEE Transactions on Industrial Informatics,* vol. 9, no. 2, pp. 1003-1016, 2012.

[22] Y. Zhang, H. Yang, and B. Xia, "Model-Predictive Control of Induction Motor Drives: Torque Control Versus Flux Control," *IEEE Transactions on Industry Applications,* vol. 52, no. 5, pp. 4050-4060, 2016.

[23] F. Wang, S. Li, X. Mei, W. Xie, J. Rodríguez, and R. M. Kennel, "Model-Based Predictive Direct Control Strategies for Electrical Drives: An Experimental Evaluation of PTC and PCC Methods," *IEEE Transactions on Industrial Informatics,* vol. 11, no. 3, pp. 671-681, 2015.

[24] M. Siami, D. A. Khaburi, M. Rivera, and J. Rodríguez, "An Experimental Evaluation of Predictive Current Control and Predictive Torque Control for a PMSM Fed by a Matrix Converter," *IEEE Transactions on Industrial Electronics,* vol. 64, no. 11, pp. 8459-8471, 2017.

[25] P. Correa, M. Pacas, and J. Rodriguez, "Predictive Torque Control for Inverter-Fed Induction Machines," *IEEE Transactions on Industrial Electronics,* vol. 54, no. 2, pp. 1073-1079, 2007.

[26] J. Retif, L.-S. Xuefang, and F. Morel, "Predictive Current Control for an Induction Motor," in *2008 IEEE Power Electronics Specialists Conference*, 15-19 June 2008 2008, pp. 3463-3468.

[27] L. Wang and L. Gan, "Integral FCS Predictive Current Control of Induction Motor Drive," *IFAC Proceedings Volumes,* vol. 47, no. 3, pp. 11956-11961, 2014/01/01/ 2014.

[28] M. Mamdouh and M. A. Abido, "Efficient Predictive Torque Control for Induction Motor Drive," *IEEE Transactions on Industrial Electronics,* vol. 66, no. 9, pp. 6757-6767, 2019.

[29] M. Uddin, S. Mekhilef, M. Nakaoka, and M. Rivera, "Model predictive control of induction motor with delay time compensation: An experimental assessment," in *2015 IEEE Applied Power Electronics Conference and Exposition (APEC)*, 2015: IEEE, pp. 543-548.

[30] L. Sheng, D. Li, and Y. Ji, "Two-Vector FCS-MPC for Permanent-Magnet Synchronous Motors Based on Duty Ratio Optimization," *Mathematical Problems in Engineering,* vol. 2018, 2018.

[31] Y. Zhang and Y. Bai, "An efficient two-vector-based model predictive control for induction motor drives," in *2017 20th International Conference on Electrical Machines and Systems (ICEMS)*, 11-14 Aug. 2017 2017, pp. 1-6.

[32] Y. Zhang and H. Yang, "Two-Vector-Based Model Predictive Torque Control Without Weighting Factors for Induction Motor Drives," *IEEE Transactions on Power Electronics,* vol. 31, no. 2, pp. 1381-1390, 2016.

[33] Y. Liu, S. Cheng, Y. Zhao, J. Liu, and Y. Li, "Optimal two-vector combination-based model predictive current control with compensation for PMSM drives," *International Journal of Electronics,* vol. 106, no. 6, pp. 880-894, 2019.

[34] Y. Xu, H. Li, J. Ren, and Y. Zhang, "Three-vector-based model predictive current control with disturbance feedforward compensation," *Journal of Power Electronics,* 2020.

[35] S. Kang, J. Soh, and R. Kim, "Symmetrical Three-Vector-Based Model Predictive Control With Deadbeat Solution for IPMSM in Rotating Reference Frame," *IEEE Transactions on Industrial Electronics,* vol. 67, no. 1, pp. 159-168, 2020.

[36] M. Aguirre, S. Kouro, C. A. Rojas, J. Rodriguez, and J. I. Leon, "Switching Frequency Regulation for FCS-MPC Based on a Period Control Approach," *IEEE Transactions on Industrial Electronics,* vol. 65, no. 7, pp. 5764-5773, 2018.

[37] M. Tomlinson, T. Mouton, R. Kennel, and P. Stolze, "Model predictive control with a fixed switching frequency for a 5-level flying capacitor converter," in *2013 IEEE ECCE Asia Downunder*, pp. 1208-1214,3-6 June 2013 2013.

[38] H.-J. Yoo, T.-T. Nguyen, and H.-M. Kim, "MPC with Constant Switching Frequency for Inverter-Based Distributed Generations in Microgrid Using Gradient Descent," *Energies,* vol. 12, no. 6, p. 1156, 2019.